Spectroscopic reflectometry for characterization of Through Silicon Via profile of Bosch etching process

Joachim Bauer, Oksana Fursenko, Steffen Marschmeyer, Friedhelm Heinrich, Francesco Villasmunta, Claus Villringer, Christoph Zesch, and Sigurd Schrader

Citation: Journal of Vacuum Science & Technology B **37**, 062205 (2019); doi: 10.1116/1.5120617
View online: https://doi.org/10.1116/1.5120617
View Table of Contents: https://avs.scitation.org/toc/jvb/37/6
Published by the American Vacuum Society

Spectroscopic reflectometry for characterization of Through Silicon Via profile of Bosch etching process

Joachim Bauer,[1,a)] Oksana Fursenko,[2] Steffen Marschmeyer,[2] Friedhelm Heinrich,[1] Francesco Villasmunta,[1,2,3] Claus Villringer,[1] Christoph Zesch,[1] and Sigurd Schrader[1]
[1]*Technical University of Applied Sciences Wildau, Hochschulring 1, 15745 Wildau, Germany*
[2]*IHP—Leibniz-Institut für innovative Mikroelektronik, Im Technologiepark 25, 15236 Frankfurt (Oder), Germany*
[3]*Department of Industrial Engineering, University of Rome, Tor Vergata, 00133 Rome, Italy*

(Received 24 July 2019; accepted 30 September 2019; published 19 November 2019)

Through Silicon Via (TSV) technology is a key in 3D integration of circuits by the creation of interconnects using vias, which go through the full silicon wafer. Typically, a highly-selective Bosch Si etch process is used. It is characterized by a high etch rate at a high aspect ratio, whereby scallops on the sidewalls are generated. In this work, square via arrays with dimensions from 3 to 50 μm and up to 300 μm depth were fabricated and analyzed by spectroscopic reflectometry. The reflectometric data are compared to simulations by a novel theoretical approach. In order to simulate the reflectance spectra of TSV arrays, a combination of 2D and 3D rigorous coupled wave analysis was applied. Besides the via depth, the sidewall angle and the corner radius of the bottom profile were considered in the model. The general requirements on spectral resolution in TSV metrology are discussed. *Published by the AVS.*
https://doi.org/10.1116/1.5120617

I. INTRODUCTION

Generally, Through Silicon Vias (TSVs) are formed by etching vertical vias and filling them with conductive materials, such as copper or tungsten.[1] TSV technology has opened up new possibilities of 3D integration of microelectromechanical systems in different fields, like photonic circuits, microfluidic devices, or electrical grounding of CMOS and BiCMOS devices.[2,3] It offers higher packaging density and lower costs for advanced 3D integration. It can be advantageous further in terms of reducing bending stress effects due to the wafer thinning process as well as thermal stress inside the TSV caused by the mismatch of thermal expansion of Si and the filling material.[4,5]

Via etching is a critical step in TSV integration impacting isolation, metallization, and wafer thinning. Typically, the Bosch process is used, providing high selectivity and etch rates required for high aspect ratio (AR) deep silicon etching.[6] The Bosch process includes repeated alternating isotropic dry etching and sidewall passivation steps. By this way, a series of scallops are generated on the sidewalls which may reduce the reliability of the devices, by showing leakage currents, thermo-mechanical stress, or slow device response.

For 3D stacking based on TSVs, a tapered profile geometry of the vias is required for conformal deposition of dielectric materials followed by filling with conductive materials like polysilicon or metal for direct dye interconnections.[7,8] Therefore, the etch profile must be well controlled to ensure that all requirements for 3D interconnects are fulfilled. Usually, secondary electron microscopy (SEM) cross section image analysis is applied. But SEM is destructive, time consuming, and depends on the cutting technique. Optical interferometry and reflectometry are the main nondestructive metrological methods for this purpose.[9–11] But, their application is limited by ever decreasing dimensions and high ARs of TSVs due to the requirement of obtaining a measurable signal of reflected light from the bottom of the TSVs. As we have shown recently,[12] the reflection data for patterns with aspect ratios of up to 35:1 could be safely evaluated by our DeepView setup. Besides, the scallop sizes could be estimated from light diffraction caused by the side wall scallops. The rigorous coupled wave analysis (RCWA)[13–15] was applied for top and bottom critical dimension (CD) and scallop amplitude[12,16,17] evaluations.

In the current work, a novel theoretical approach was used based on the combination of 2D and 3D RCWA. This model is used to analyze the influence of the side wall angle and the corner radius of the bottom profile of the vias on the reflection spectra, in addition to the depth of the vias. We provide an estimate for the requirements on the spectral resolution to archive a sufficiently high degree of modulation of the interference signal for safe frequency determination.

II. EXPERIMENTAL AND MODELING

Square via arrays with lateral dimensions (CD) of 3, 5, 10, and 50 μm and up to 300 μm depth were generated by a highly-selective Bosch etch process, using SF_6 and C_4F_8/O_2 chemistry and an SiO_2 hard mask.[18] All measurements were carried out by our own experimental DeepView reflectometry setup[12] at a numerical aperture (NA) of 0.01, a spot size of 250 μm, and a spectral range of 400–600 nm. In order to

Note: This paper is part of the Conference Collection: 8th International Conference on Spectroscopic Ellipsometry 2019, ICSE.
[a)]Electronic mail: jobauer@th-wildau.de

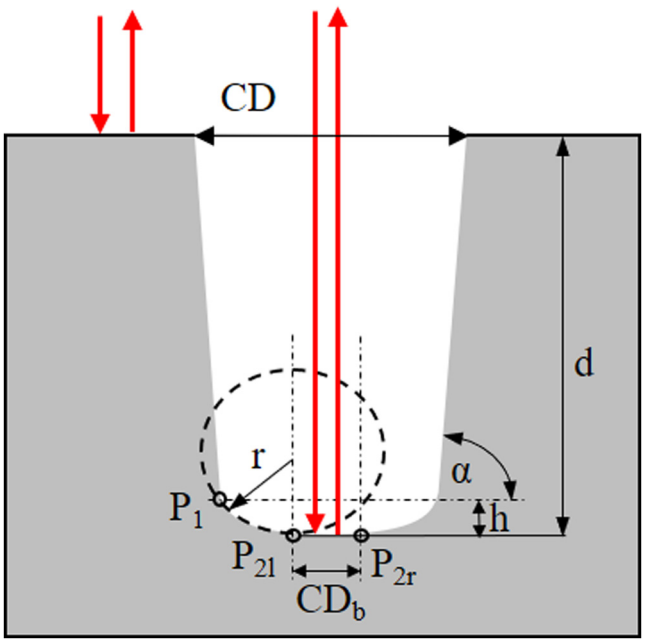

FIG. 1. Schematics of the TSV profile, reflection signal, and parameters for RCWA and RT model simulations. The bottom critical dimension CD_b is assumed as a flat area.

demonstrate the effect of the spectral resolution on the interferometric signals, different spectrometers with a wavelength resolution in the range of 0.1–2 nm were used.

The interference signal is generated by a superposition of waves reflected from the TSV's top and bottom surfaces. The frequency of the interference signal provides the TSV depth extracted from the Fourier Transform analysis.[11,12,16,17] Our RCWA-Maxwell solver[15] uses the Fourier expansion of the field and periodic relative permittivity. In order to save the computation time caused by the high wavelength resolution, a full 3D treatment was avoided. Instead, slicing of the TSV structure in distinct horizontal slabs was introduced, where the height of the slabs could be adapted to the considered geometry. Basically, this method relies on the transformation of Maxwell's equations within the slice into a system of differential equations for the transversal field components. Then, these equations are Fourier factorized and solved by means of Eigenvalue decomposition.

This procedure can be compared with a ray tracing (RT) model. Although this model is very simple, it does not take into account the diffraction as well as sophisticated considerations of via and bottom profiles. In this case, the reflectance R for infinitely coherent light can be obtained by geometrical relations,

$$R = ar_{Si}^2 + f(1-a)r_{Si}^2 + 2\sqrt{af(1-a)}r_{Si}^2\cos\left(\frac{4\pi d}{\lambda}\right), \qquad (1)$$

where r_{Si} is the reflectance coefficient of the silicon, d is the via depth, and λ is the wavelength.[10] The coefficients a and $(1-a)$ describe the ratio of the illuminated silicon top surface and the via opening, respectively, with respect to the total illuminated area. In our case, $a \approx 0.75$. The ratio of the effective illumination area in the via bottom to the via top opening area is expressed as f and for a given NA, $f = (D/\mathrm{CD})$,[2] where D is the effective diameter of the bottom illuminated area and CD is the critical dimension. In the following, the interference contrast, defined as $C = (R_{max} - R_{min})/(R_{max} + R_{min})$, is calculated in both the models (RCWA and RT) and compared with the experimental results, where C_{exp} and C_c are the experimental and simulated contrast values.

The 2D RCWA simulation of normalized interference contrast $C_c/C_c(\alpha = 90°)$ is used for a very deep trapezoidal TSV structure with the side wall slope α and smooth and flat TSV bottom. The interference contrast calculation $C_c(r)$ of reflection properties of the bottom profile with height h and radius r is done by 3D RCWA, whereas in this case we neglect the trapezoidal structure and approximate it by a vertical profile. The expected contrast is then given by a multiplication of both the values,

$$C_c = C_c(r)C_c(\alpha)/C_c(\alpha = 90°). \qquad (2)$$

The consideration of the corner radius in the RCWA calculation is based on the determination of points P_1 and P_{21} at

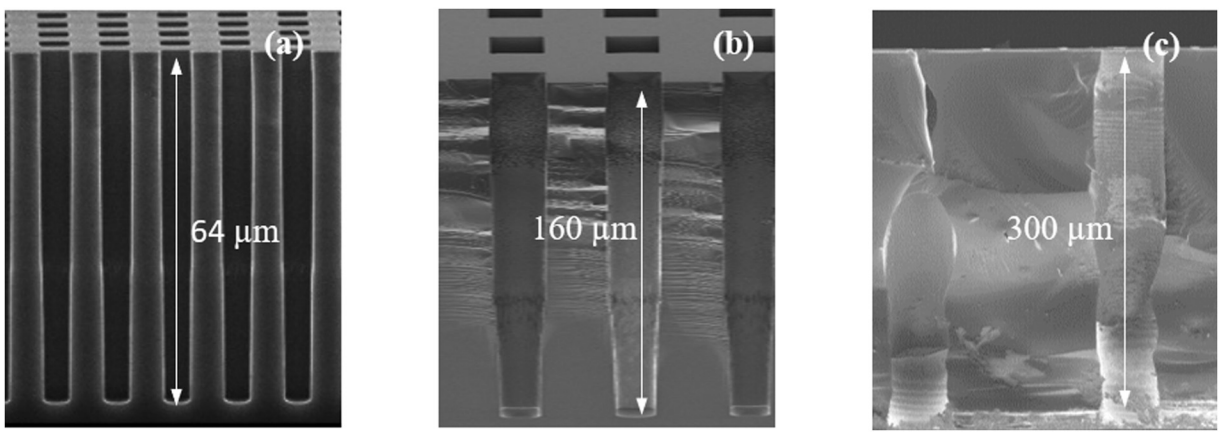

FIG. 2. SEM cross sections of the arrays with (a) CD = 5 μm, via depth d = 64 μm, period p = 10 μm, (b) CD = 10 μm, d = 160 μm, p = 20 μm, and (c) CD = 50 μm, d = 300 μm, p = 150 μm.

given r and h, as shown in Fig. 1. The bottom profile from P_{2l} to P_{2r} is denoted as CD_b and is assumed as a flat area.

III. RESULTS AND DISCUSSION

The etched profiles and the corresponding measured reflectances are shown in Figs. 2 and 3. The depths and other profile parameters, such as the sidewall angle and the profile radius, affect the degree of modulation. As a precondition for safe depth measurement, the interference contrast C_{exp} must be sufficiently high to be clearly distinguished from the noise by FFT analysis. This requires a sufficiently high coherence length of the light field and hence sufficiently high spectral resolution $\Delta\lambda$ of the measurement setup.

The influence of $\Delta\lambda$ on the reflection and the corresponding power spectra is clearly visible. The modulation depth (interference contrast) is distinctly pronounced at lower $\Delta\lambda$, whereas at higher $\Delta\lambda$ the modulation amplitude is hardly distinguished from noise. Accordingly, the power spectrum, which was generated over the full spectral range, shows a much higher amplitude at lower $\Delta\lambda$. As deduced from the time frequency uncertainty relation $\Delta\tau\Delta\nu \sim 1$, the coherence length l_c of a wave train at a certain wavelength λ can be estimated by $l_c = \lambda^2/\Delta\lambda$. Theoretically, the interference effects should be detectable when $l_c > 2d$. Figure 3(a) shows the wavelength dependence of the interference signals for 60 μm TSV depth. For $\Delta\lambda = 1.2$ nm spectrometer resolution, $l_c \sim 208\,\mu$m, which is about twice the TSV depth, and the interference is still detectable for wavelengths >500 nm. At $\Delta\lambda = 0.2$ nm, when $l_c \gg 2d$, the modulation degree is significantly improved, since a larger number of phase-correlated oscillations overlap. For 160 μm deep TSV [Fig. 3(b)], a

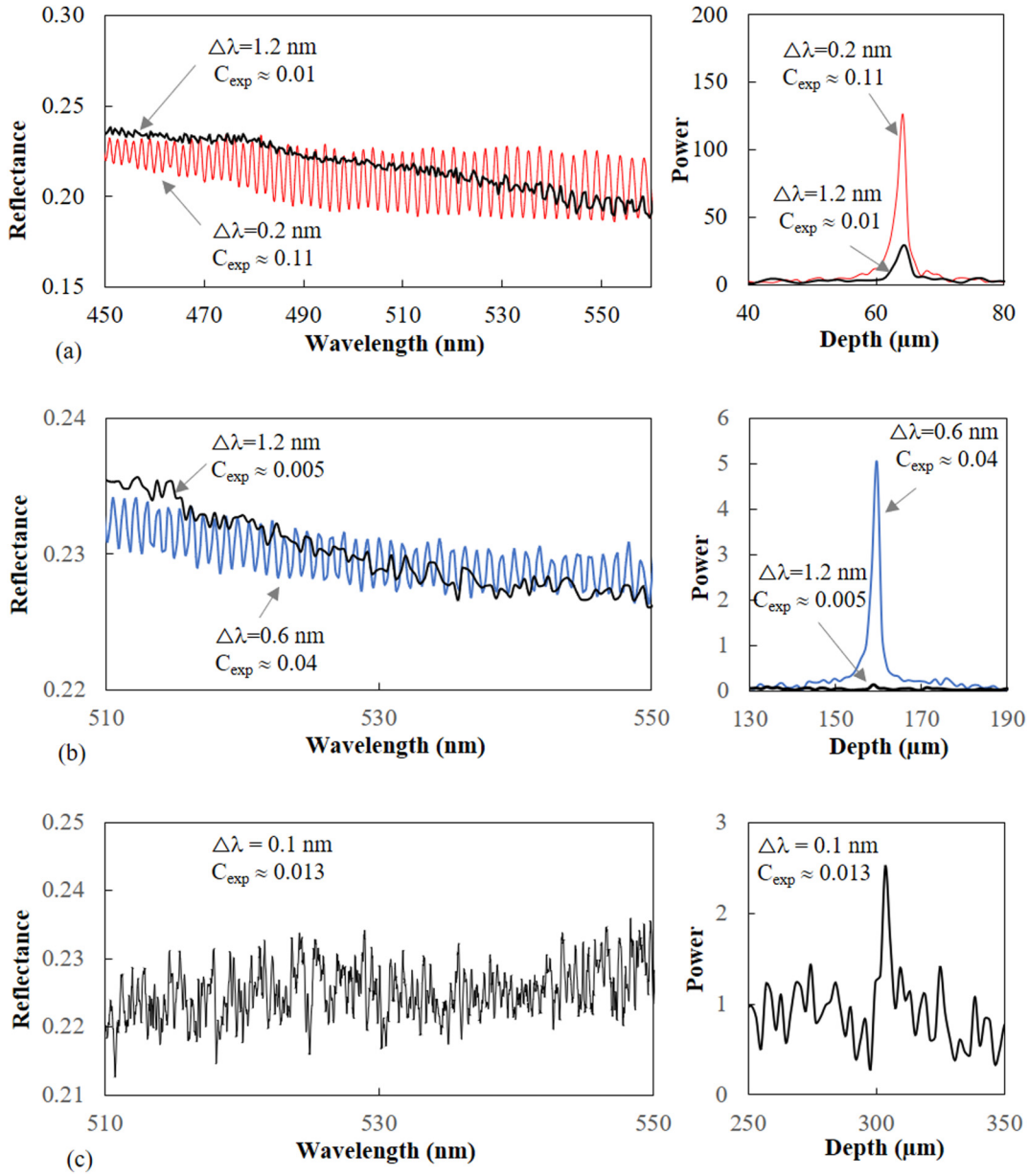

FIG. 3. Measured reflectance and Fourier analysis for the etch depth d evaluation of the arrays with (a) CD = 5 μm, via depth d = 64 μm, period p = 10 μm, and spectral resolution $\Delta\lambda$=0.2 and 1.2 nm, (b) CD = 10 μm, d = 160 μm, p = 20 μm, and $\Delta\lambda$=0.6 and 1.2 nm, and (c) CD = 50 μm, d = 300 μm, p = 150 μm, and $\Delta\lambda$ = 0.1 nm.

resolution of 1.2 nm is no longer sufficient to perform a reliable depth measurement, while at $\Delta\lambda = 0.6$ nm the modulation frequency could be clearly evaluated by the Fourier analysis. Figure 3(c) shows the reflection signals for 300 μm TSV depth recorded at 0.1 nm resolution. Although $l_c \sim 2500\,\mu$m clearly exceeds $2d$, the contrast value is rather small, which indicates that in addition to the spectral resolution, the amplitude of the oscillations is influenced by other parameters such as the inclination angle, bottom profile, CD, and bottom surface roughness of the TSV as well as by the interaction of the electric field with the side wall scallops. Of

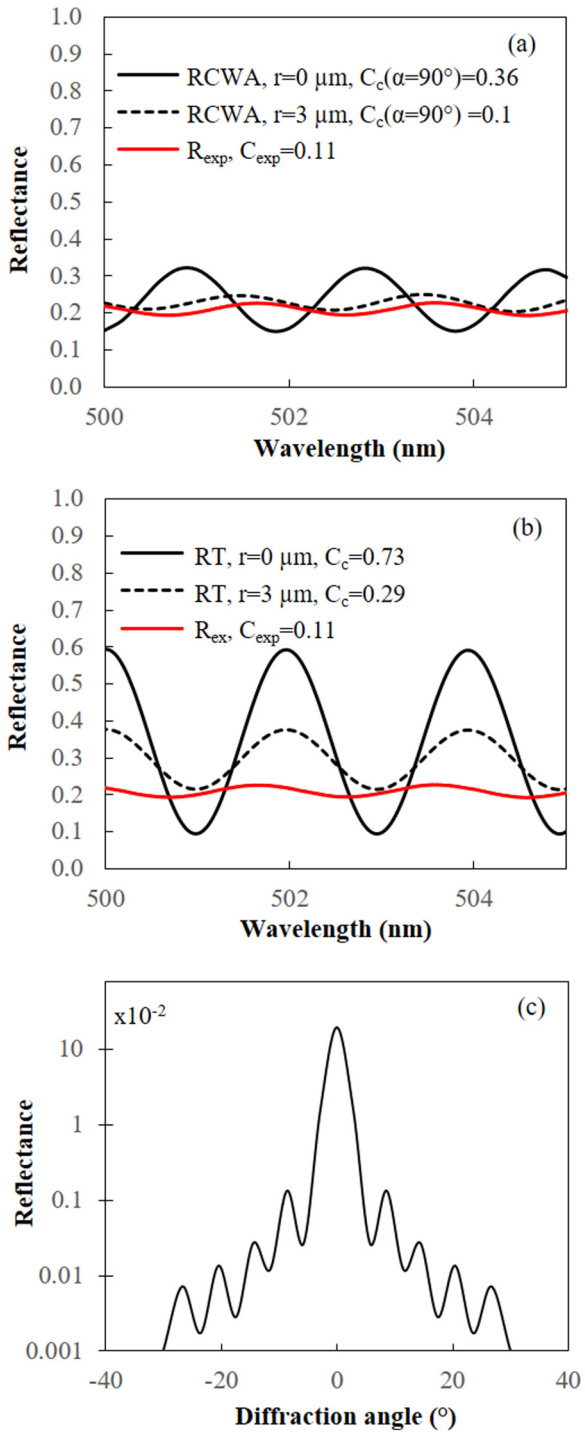

FIG. 4. RCWA (a) RT model (b) simulations and measured reflections with a spectral resolution $\Delta\lambda = 0.2$ nm for the TSV array with CD $\approx 5\,\mu$m, period $p = 10\,\mu$m, depth $d = 64\,\mu$m and bottom profile radius $r = 3\,\mu$m, height $h = 1\,\mu$m and sidewall angle $\alpha = 90°$ compared to a smooth profile ($r = 0\,\mu$m); (c) RCWA angle-dependent light distribution for $r = 3\,\mu$m, $h = 1\,\mu$m, $\alpha = 90°$, and $\lambda = 500$ nm.

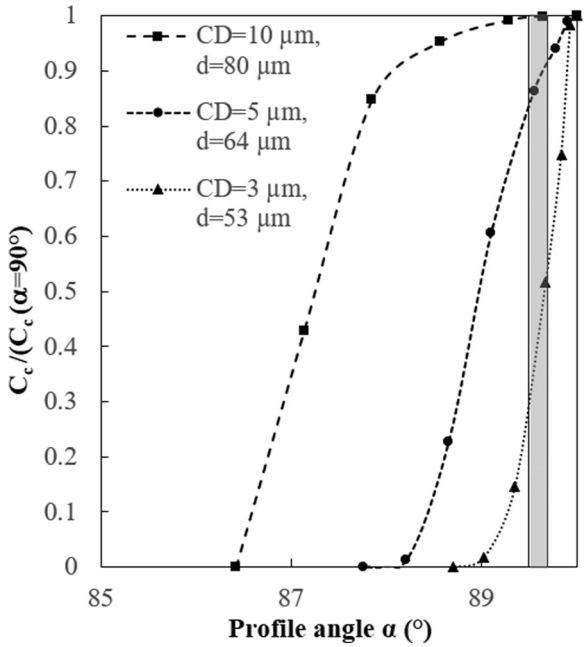

FIG. 5. Normalized interference contrast $C_c/C_c(\alpha = 90°)$ as a function of the sidewall angle α simulated by two-dimensional rigorous coupled wave analysis (2D RCWA). The simulated interference contrast (C_c) for period $p = 20\,\mu$m is normalized to $C_c(\alpha = 90°) = 0.96$, C_c for $p = 10\,\mu$m is normalized to $C_c(\alpha = 90°) = 0.79$, and C_c for $p = 6\,\mu$m is normalized to $C_c(\alpha = 90°) = 0.23$. The gray rectangle in the diagram represents the typical sidewall angles after the Bosch process.

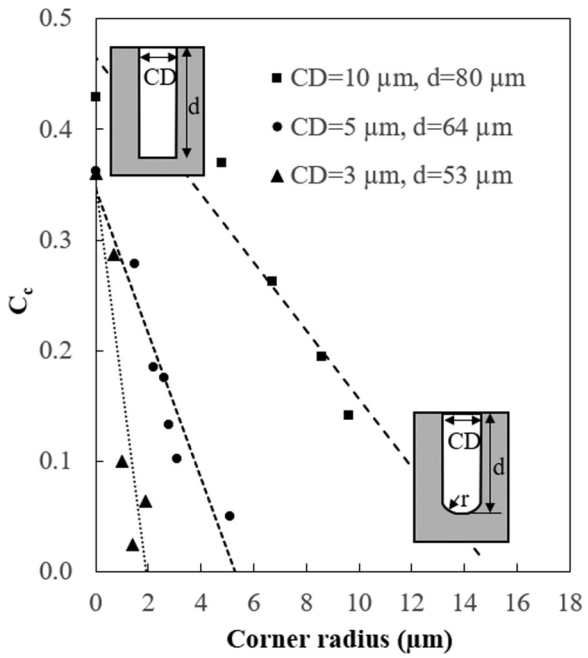

FIG. 6. Interference contrast C_c as a function of the corner radius r calculated with three-dimensional rigorous coupled wave analysis (3D RCWA) for the sidewall angle $\alpha = 90°$.

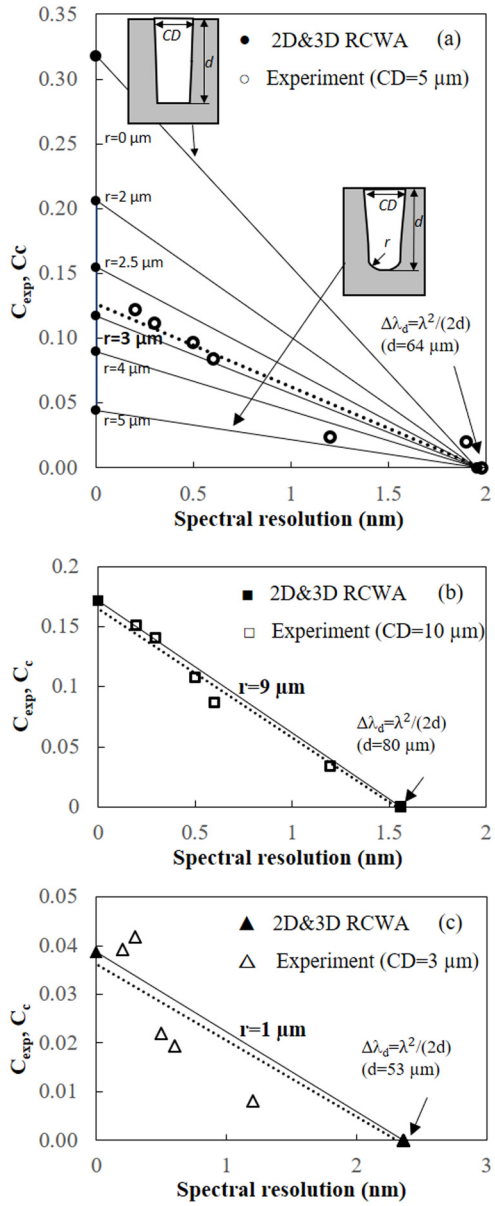

FIG. 7. Simulated C_c and measured C_{exp} interference contrasts at different spectral resolutions and (a) CD = 5 μm, (b) CD = 10 μm, and (c) CD = 3 μm arrays (dashed line: linear regression of the measured interference contrast C_{exp}). The point C_c at spectral resolution $\Delta\lambda = 0$ provides the contrast at coherent superposition. The dashed line depicts the linear regression of the measured interference contrast C_{exp}.

course, the evaluation depends strongly on the signal-to-noise ratio (SNR) of the acquired signal, which in the latter case is significantly lower due to the limited light throughput of the system.

In Fig. 4(a), the RCWA simulation is shown for a flat and a rounded bottom profiles, together with the experimental reflectance data for a rounded bottom profile according to Fig. 8. The simulation fits the experimental data (dashed line) very well. In contrast, the RT calculations based on a pure geometric view, described by Eq. (1), significantly overestimate the contrast values [Fig. 4(b)]. The large difference in reflection and contrast between the two models is suggested to be mainly caused by diffraction effects and the interaction of the electromagnetic waves with the via sidewalls. As shown in Fig. 4(c), the diffraction leads to a quite large angular distribution of the reflected light. Thus, a considerable part of the reflected intensity is lost due to the limited aperture of the optics. It should be mentioned here that the diffraction pattern contains additional information on profile parameters, which, however, was not measurable with the present setup. In practice, deviations from 90° side wall angle lead to a further reduction in C_c. Figure 5 shows the normalized interference contrast $C_c/C_c(\alpha = 90°)$ as a function of the sidewall angle and a flat bottom profile simulated by 2D RCWA. It is shown that for CD > 10 μm, the sidewall angle of the TSV process hardly affects the interference contrast. The C_c values as a function of bottom corner radius for vertical profiles ($\alpha = 90°$) are presented in Fig. 6. Figures 7 and 8 demonstrate a good matching of the RCWA profile simulation versus corner radius with the experimental SEM measurements of corner radius. Figure 7 shows the calculated contrast values C_c for infinite coherence and experimentally determined contrast C_{exp} as a function of the spectral resolution $\Delta\lambda$, where the limiting resolution is given by $\Delta\lambda_d = \lambda^2/(2d)$. If $\Delta\lambda > \Delta\lambda_d$, there is no phase correlation between the waves reflected from the top and the via bottom, and hence no measurable interference effects can appear. C_{exp} depends approximately linearly on the spectral resolution; thus, the required resolution $\Delta\lambda$ can be described as

$$\Delta\lambda = \Delta\lambda_d\left(1 - \frac{C_r}{C_c}\right) = \frac{\lambda^2}{2d}\left(1 - \frac{C_r}{C_c}\right), \tag{3}$$

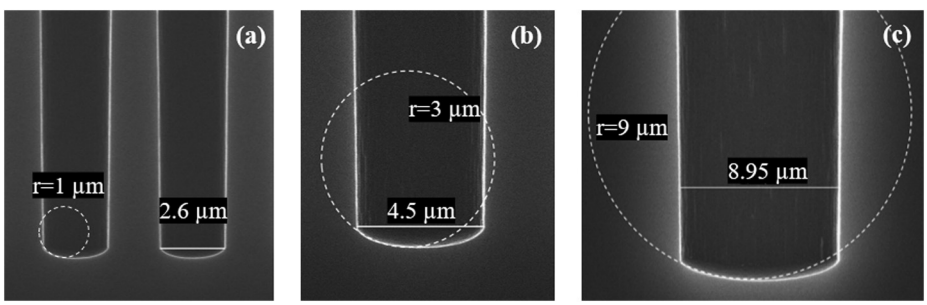

FIG. 8. SEM cross sections of TSV bottom. (a) Bottom profile radius $r \approx 1\,\mu$m for CD = 3 μm, (b) $r \approx 3\,\mu$m for CD = 5 μm, and (c) $r \approx 9\,\mu$m for CD = 10 μm arrays. The drawn radii result from the fit of the measured and calculated reflection when using spectrometers with different resolutions as shown in Fig. 7.

TABLE I. Required spectral resolution $\Delta\lambda$ for TSV.[a]

TSV depth (μm)	TSV CD (μm)	RCWA coherent contrast C_c	C_r	$\Delta\lambda_d = \lambda^2/(2d)$ (nm)	Required spectral resolution $\Delta\lambda$ (nm)
64	5	0.1	0.01	1.95	1.8
160	10	0.23	0.01	0.78	0.7
300	50	0.42	0.01	0.42	0.3

[a]C_c is the interference contrast calculated by 3D RCWA ($\alpha = 90°$), C_r is the needed interference contrast under given experimental conditions, and $\Delta\lambda_d$ is the resolution at the coherence length $l_c = 2d$ for $\lambda = 500$ nm.

where C_r ($<C_c$) is the relative noise amplitude, defined as the mean statistical fluctuation amplitude with respect to the averaged total detector signal, equivalent to the inverse SNR value of the setup. Equation (3) describes the fact that, in practice, the resolution of the spectrometer must always be higher than the theoretical limit $\lambda^2/(2d)$. For a given SNR, the required minimum resolution depends strongly on the profile parameters, side wall inclination angle α, and bottom curvature, approximated by a rounded radius r (see Fig. 1). According to Eq. (2), C_c depends on both the radius of curvature r of the bottom profile and the inclination angle. In order to make simple estimates possible, our calculations regarding the minimum required spectrometer resolution were based on $\alpha = 90°$, a simplification which in the cases considered in this paper is not too far from reality (see Fig. 4). Assuming $C_r \sim 0.01$ leads to $\Delta\lambda \sim 0.9\lambda^2/(2d)$, taking the calculated C_c values from Table I, which summarizes the results obtained from Eq. (3). Figure 7 shows the experimental contrast values for different spectrometer resolutions and three different hole parameters related to the SEM images in Fig. 8. The calculated values for infinite coherence ($\Delta\lambda = 0$) and limiting coherence $\Delta\lambda_d$ are also indicated in Fig. 7.

IV. CONCLUSIONS

Spectroscopic reflectometry was applied for characterizing TSV profiles generated by a Bosch etching process. The influence of TSV depths, side walls, bottom profiles, and spectral resolution on the interference contrast could be simulated by a new approach, combining 2D and 3D rigorous coupled wave analysis (RCWA). In this paper, the model was applied to experimental data, showing that the influence of different bottom profiles on the reflection spectra could be adequately described. The respective results of our simulation are in good agreement with the SEM cross sections of the vias. This study, in combination with our previous work referred to in this paper, suggests that spectroscopic reflectometry can be a powerful tool for characterizing high aspect ratio TSVs. In combination with appropriate modeling, a more complex topology analysis, including bottom profile, sidewall angles, and scallops, appears feasible.

[1]W. Rhines, *3D-IC Challenges, GSA Memory Conference*, San Jose, CA, 31 March 2011 (31 March 2011).
[2]D. Gerke, NASA 2009, Body of Knowledge (BoK): Through-Silicon via Technology, JPL Publication 09-28 11, 2009.
[3]M. Wietstruck, M. Kaynak, St. Marschmeyer, C. Wipf, I. Tekin, K. Zoschke, and B. Tillack, *Proceedings of 14th Topical Meeting on Silicon Monolithic Integrated Circuits in RF Systems (SiRF 2014)*, Newport Beach, CA (19–23 January, 2014), p. 83.
[4]H. B. Chang *et al.*, *IEEE Symposium on VLSI Technology*, June 2012 (IEEE, San Francisco, CA, 2012), p. 173.
[5]S. Warnat, "Technologies for the integration of Through Silicon Vias in MEMS packages," Thesis (Flintberg, 2009).
[6]F. Laermer and A. Schilp, German patent DE4241045C1 (5 December 1992).
[7]D. S. Tezcan, K. De Munck, N. Pham, O. Luhn, A. Aarts, P. De Moor, K. Baert, and Ch. Van Hoof, *Proceedings of 8th Conference IEEE 2006 Electronics Packaging Technology*, Singapore, 6–8 Dec. 2006 (IEEE, Singapore, Singapore, 2006), p. 22.
[8]W. H. Teh *et al.*, 2009 *IEEE International Conference on 3D System Integration: 3DIC 2009*, San Francisco, CA, 28–30 September 2009 (IEEE, San Francisco, CA, 2009), p. 222.
[9]V. Vartanian, R. A. Allen, L. Smith, K. Hummler, S. Olson, and B. Sapp, J. Micro/Nanolithogr. MEMS MOEMS **13**, 011206 (2014).
[10]Yi-Sha Ku, K.Ch. Huang, and W. Hsu, Opt. Express **19**, 5993 (2011).
[11]O. Fursenko, J. Bauer, S. Marschmeyer, and H.-P. Stoll, Microelectron. Eng. **139**, 70 (2015).
[12]J. Bauer *et al.*, Proc. SPIE **10329**, 103293J-1 (2017).
[13]M. G. Moharam, D. A. Pommet, E. B. Grann, and T. K. Gaylord, J. Opt. Soc. Am. A **12**, 1077 (1995).
[14]Lifeng Li, J. Opt. Soc. Am. A **10**, 2581 (1995).
[15]See www.unigit.net for the used software.
[16]O. Fursenko, J. Bauer, and S. Marschmeyer, Microelectron. Eng. **122**, 25 (2014).
[17]O. Fursenko, J. Bauer, and S. Marschmeyer, Proc. SPIE **9890**, 15 (2016).
[18]S. Marschmeyer, J. Berthold, A. Krüger, M. Lisker, A. Scheit, S. Schulze, A. Trusch, M. Wietstruck, and D. Wolansky, Microelectron. Eng. **137**, 153 (2015).